Supplementary material

Elemental composition and source apportionment of fine and coarse particles at traffic and urban background locations in Athens, Greece

Georgios Grivas[1,2 *], Stavros Cheristanidis[2], Archontoula Chaloulakou[2], Petros Koutrakis[3], Nikos Mihalopoulos[1,4]

[1] *Institute for Environmental Research and Sustainable Development, National Observatory of Athens, 15236, Athens, Greece*

[2] *School of Chemical Engineering, National Technical University of Athens, 15780, Athens, Greece*

[3] *Department of Environmental Health, Harvard T.H. Chan School of Public Health, Boston, MA, USA*

[4] *Environmental Chemistry Processes Laboratory, Department of Chemistry, University of Crete, 71003, Heraklion, Greece*

*Corresponding author. *E-mail address:* ggrivas@mail.ntua.gr

Table S1: Detection limits (DL) and percentage of samples below detection limits (BDL) for 48 elements analyzed by ED-XRF, PM concentrations and reflectance-based absorption coefficient (ABS).

Component	DL (ng m^{-3})	BDL (%)	Component	DL (ng m^{-3})	BDL (%)
PM_{10} (µg m^{-3})	1.93	0	Se	3.5	86.1
$PM_{2.5}$ (µg m^{-3})	1.48	0	Br	4.1	29.8
ABS (10^{-5} m^{-1})	0.05	0	Rb	1.8	93.0
EC (µg m^{-3})	0.30	-	Sr	0.4	57.9
Na	51.4	2.3	Y	2.4	85.4
Mg	10.2	8.6	Zr	4.1	59.9
Al	7.0	3.3	Nb	6.2	94.4
Si	21.3	3.6	Mo	3.9	77.2
P	1.8	92.7	Pd	11.9	96.3
S	0.8	1.7	Ag	1.6	93.7
Cl	3.8	9.9	Cd	4.4	96.4
K	1.6	1.7	In	15.7	95.4
Ca	5.1	1.7	Sn	13.3	84.8
Sc	3.0	98.0	Sb	8.7	84.4
Ti	2.3	11.3	Cs	24.0	96.4
V	0.4	8.3	Ba	29.0	49.7
Cr	0.7	13.9	La	13.1	91.7
Mn	2.3	14.2	Ce	38.5	89.7
Fe	3.1	1.7	Sm	17.6	84.4
Co	0.7	65.9	Eu	86.1	92.4
Ni	0.7	9.9	Tb	124.9	97.7
Cu	1.4	3.0	W	4.2	99.7
Zn	2.0	2.0	Au	6.4	92.1
Ga	1.3	93.4	Hg	8.5	92.1
Ge	2.5	92.7	Tl	2.7	92.4
As	0.9	92.4	Pb	5.4	20.9

Table S2: Spearman rank correlation coefficients (*r*) and coefficients of divergence (CoD) for pairwise inter-site comparisons of concentrations. Displaying only elements, whose correlation coefficients were found significant at the 0.05 level.

	$PM_{2.5}$		$PM_{10-2.5}$	
	r	CoD	*r*	CoD
PM	0.61	0.38	0.39	0.43
eBC	0.54	0.54	0.43	0.62
Na	0.67	0.22	0.66	0.48
Mg	0.41	0.39	0.56	0.42
Al	0.82	0.32	0.83	0.42
Si	0.82	0.37	0.85	0.43
S	0.87	0.17	0.20	0.65
Cl	0.60	0.59	0.75	0.58
K	0.47	0.31	0.69	0.45
Ca	0.42	0.60	0.48	0.59
Ti	0.56	0.54	0.68	0.52
V	0.77	0.42	0.46	0.63
Cr	0.38	0.45	0.26	0.76
Mn	0.27	0.37	0.43	0.69
Fe	0.58	0.42	0.45	0.59
Ni	0.66	0.36	0.44	0.64
Cu	0.43	0.50	0.52	0.69
Zn	0.75	0.39	0.53	0.62

Table S3: Indicative summary of PMF parameters and error estimation (EE) diagnostics

	ARI – $PM_{2.5}$	POL – $PM_{2.5}$	ARI – $PM_{10-2.5}$	POL – $PM_{10-2.5}$
PMF parameter				
N species			20	
N samples			82	
Down-weighted species [a]	Mg	Mg, Cr, Mn	Ba	Ba, V, Ni
Excluded species [b]	Br, Ba	Br, Ba	Br	Br
Added modelling uncertainty			5%	
Base Solution				
N factors	6	6	4	4
Q_{ROBUST} / Q_{EXP}	2.15	1.86	1.95	1.72
Q_{ROBUST} / Q_{EXP} (-1 factor)	2.81	2.47	2.58	2.34
Q_{ROBUST} / Q_{EXP} (+1 factor)	2.01	1.65	1.75	1.70
Species with $Q/Q_{EXP} > 3$	Zn, Ca	Zn, Ca	S, V, Ni	Ca, Na, S
r^2, Slope [c]	0.86, 0.91	0.85, 0.95	0.88, 0.98	0.85, 0.96
BS-DISP results				
% of BS factors assigned [d]	87% (Sea Salt)	88% (Sea Salt)	97%(Road Dust)	95%(Road Dust)
DISP %dQ	-0.019	-0.018	-0.001	-0.002
DISP % of factor swaps	0	0	0	0
BS-DISP Displaced species	eBC, S, K, V, Si, Cl	eBC, S, K, V, Si, Cl	Cu, Zn, Si, Cl	Cu, Zn, Si, Cl
BS-DISP %dQ	-0.495	-0.439	-0.261	-0.896
BS-DISP % of factor swaps	2	2	0	1
BS-DISP error interval ratios for factor identifying species [e]	eBC: 0.53	eBC: 0.77	Cu: 0.65	Cu: 0.71
	S: 0.77	S: 0.87	Zn: 1.07	Zn: 0.87
	K: 0.65	K: 1.03	Si: 0.80	Si: 0.63
	V: 0.57	V: 0.84	Cl: 0.26	Cl: 0.27
	Si: 0.60	Si: 0.75		
	Cl: 1.02	Cl: 1.12		

[a] Species with signal to noise ratios (S/N) values between 0.5 - 1. Uncertainty value tripled

[b] Species with signal to noise ratios (S/N) values below 0.5. Not included in PMF

[c] Estimated vs. observed, zero-intercept linear regression

[d] 100% unless otherwise indicated (from 100 bootstrap runs, $r^2 = 0.6$)

[e] Ratio of 95^{th} -5^{th} percentile difference to average concentration

Figure S1: Comparison of concentrations determined using the Harvard Impactor with an automated beta-attenuation monitor (FH 62 I-R) for PM_{10} at the ARI site. Intercept non-significant at the 0.05 level. Standard error of the slope listed in parenthesis.

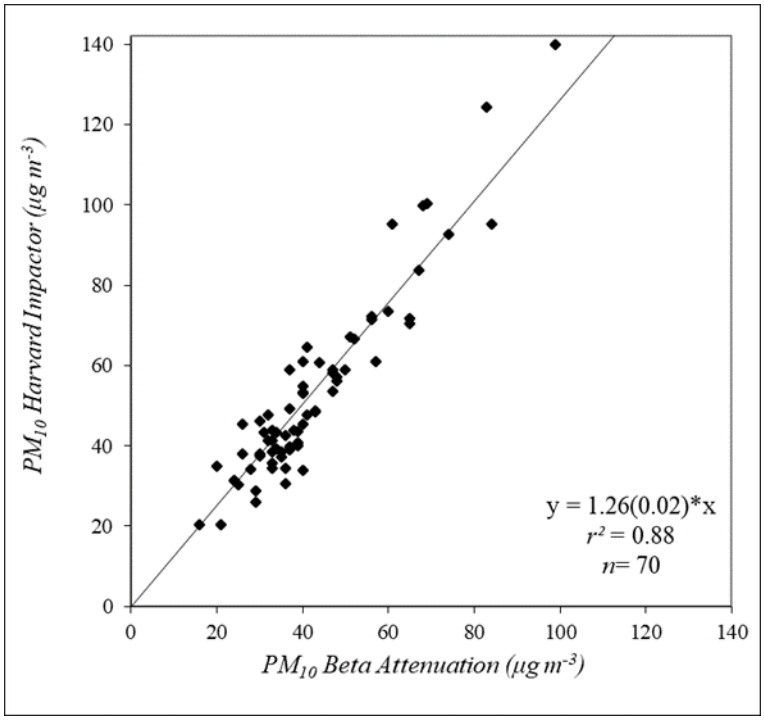

Figure S2: Calibration of reflectometer-obtained light absorption coefficient to equivalent BC (eBC) concentrations, through concurrent measurement of EC concentrations (ACPM-5400). Intercept non-significant at the 0.05 level. Standard error of the slope listed in parenthesis. Details on EC measurement can be found at Grivas et al., (2012).

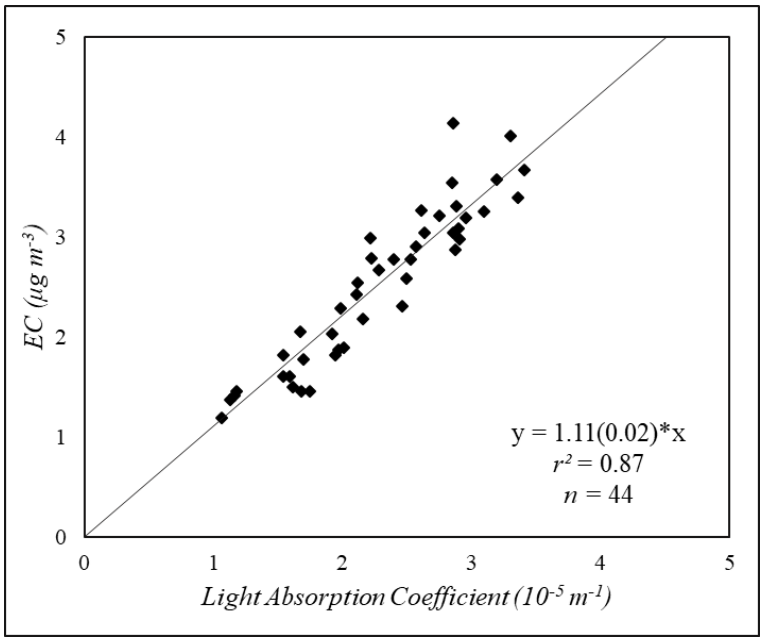

Figure S3: Enrichment factors (EF) for elements determined in a) fine and b) coarse fractions for the two sampling sites. Silicon was used as the reference element (Visser et al., 2015) and the composition of the upper crust was obtained by Wedepohl (1995). Values between below 10 are considered to indicate natural origin of the species, between 10-20 mixed anthropogenic and natural origin and over 20 a strong anthropogenic influence (Cesari et al, 2012).

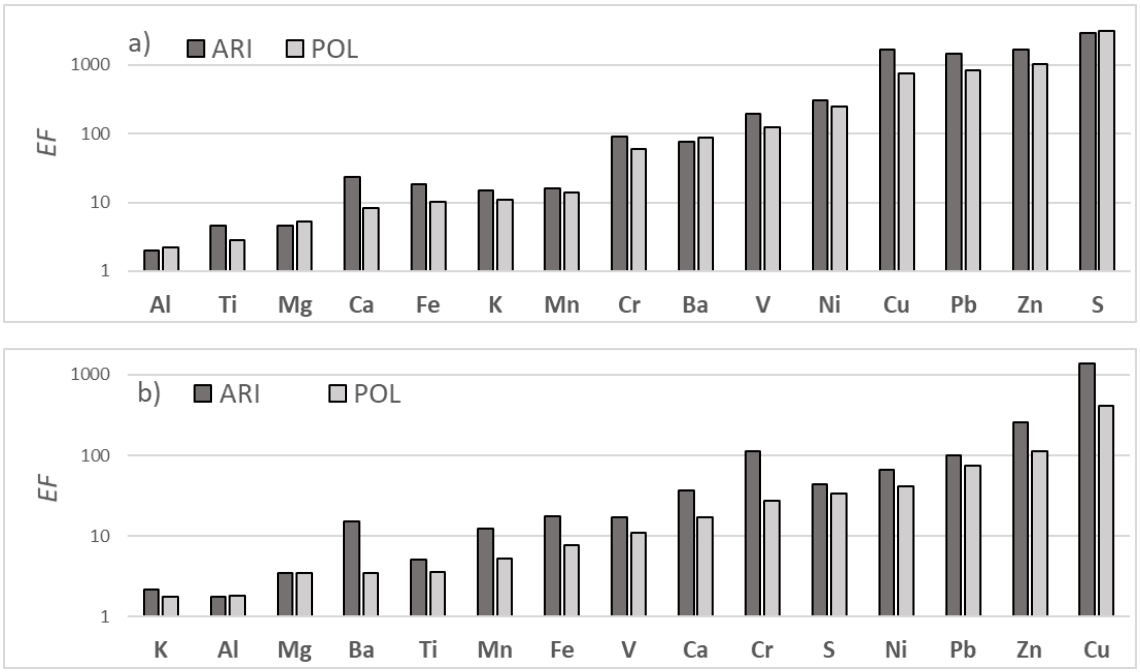

Figure S4. Spearman rank correlation coefficients for intra-site pairwise comparisons, for fine particles in ARI (a) and POL (b) and coarse particles at ARI (c) and POL (d).

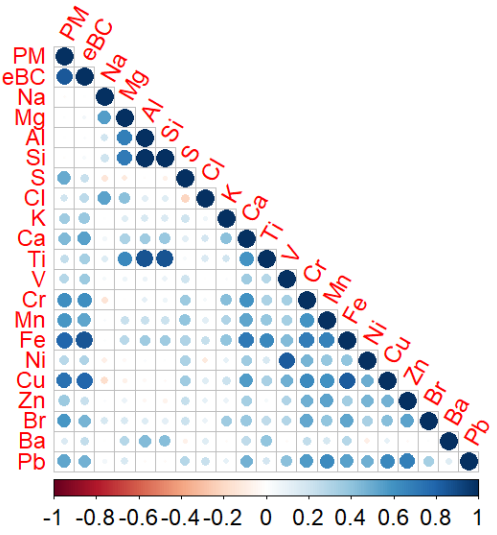

a)

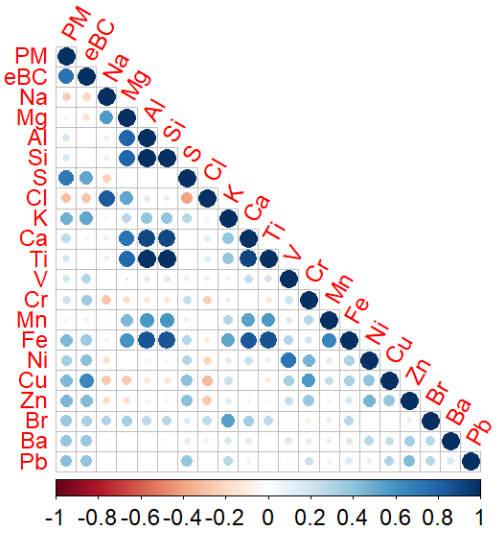

b)

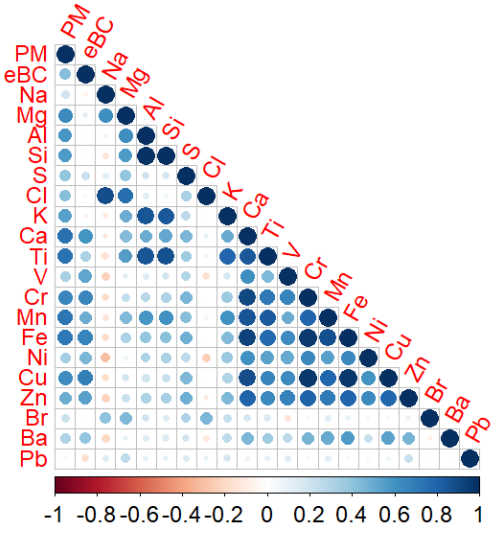

c)

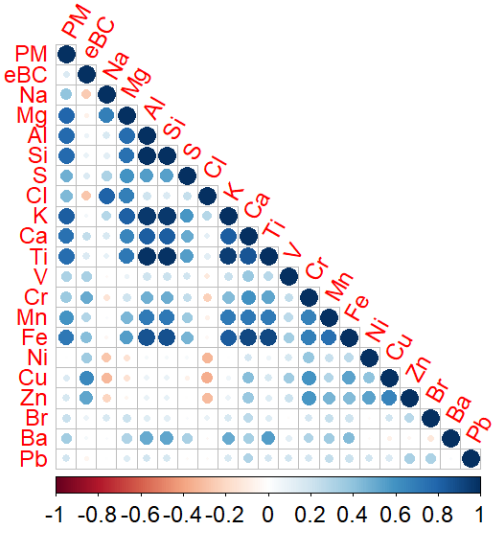

d)

Figure S5a. PMF source profiles for $PM_{2.5}$ at the roadside traffic site.

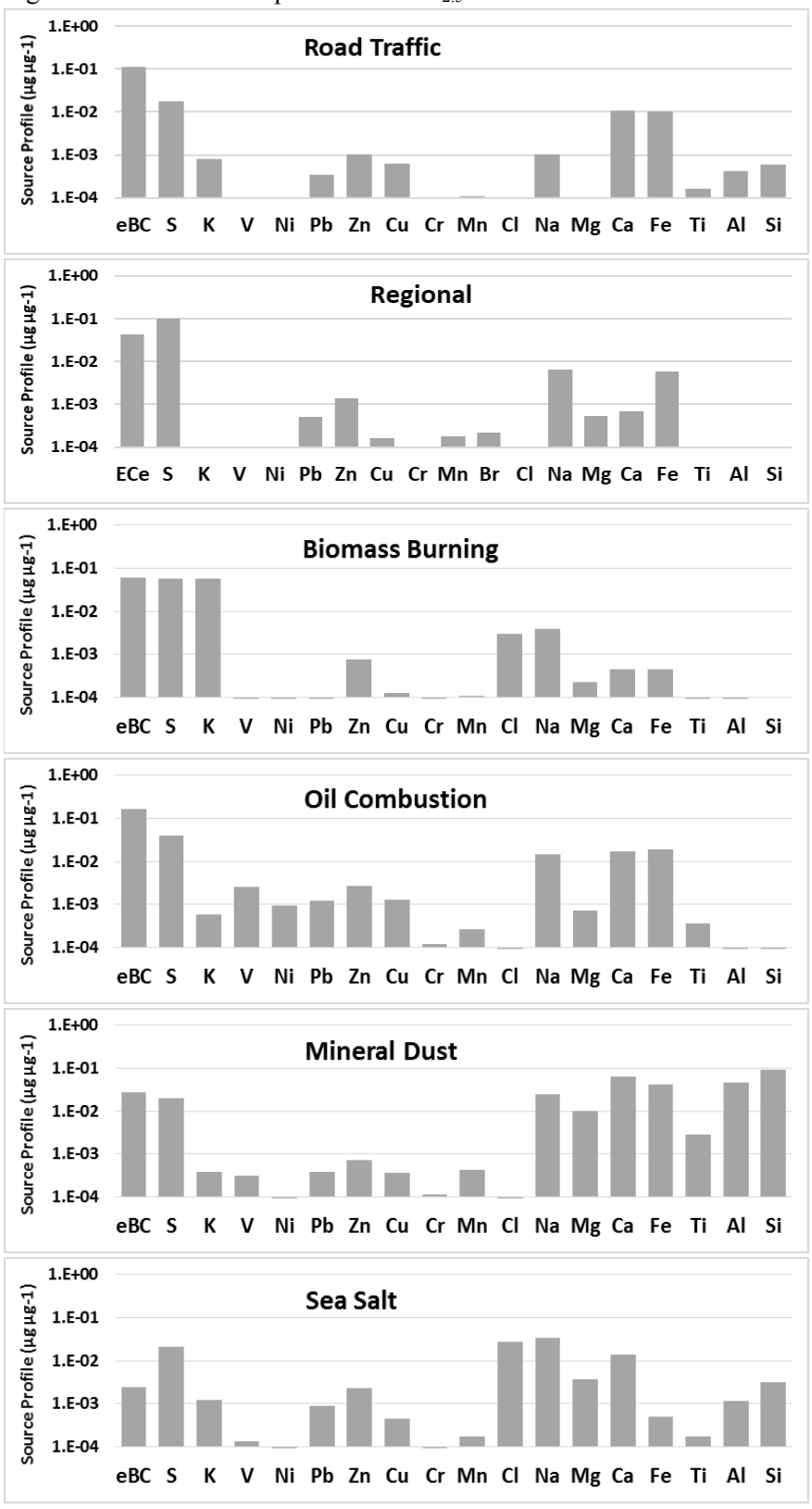

Figure S5b. PMF source profiles for $PM_{2.5}$ at the urban background site.

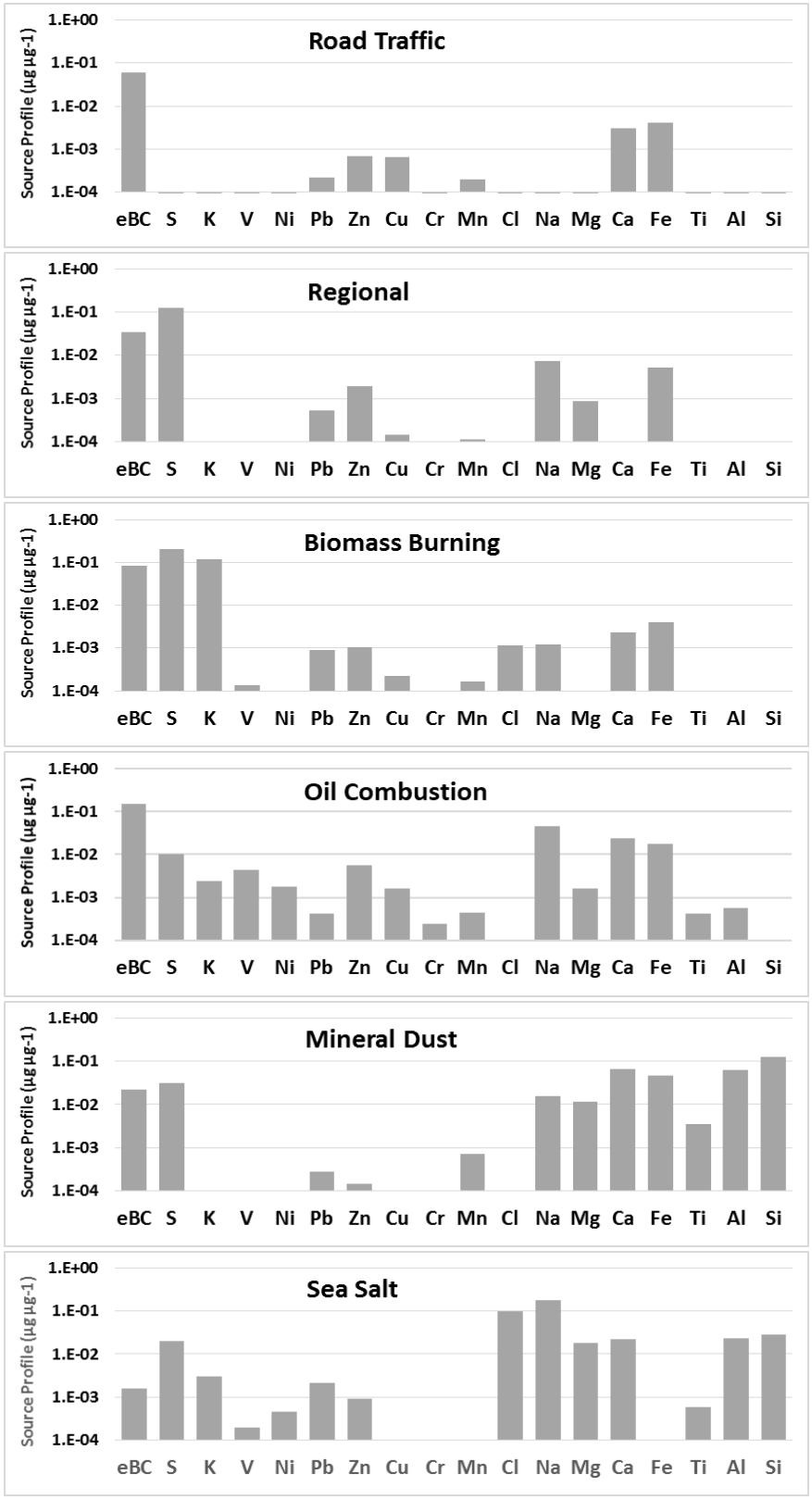

Figure S5c. PMF source profiles for $PM_{10-2.5}$ at the roadside traffic site.

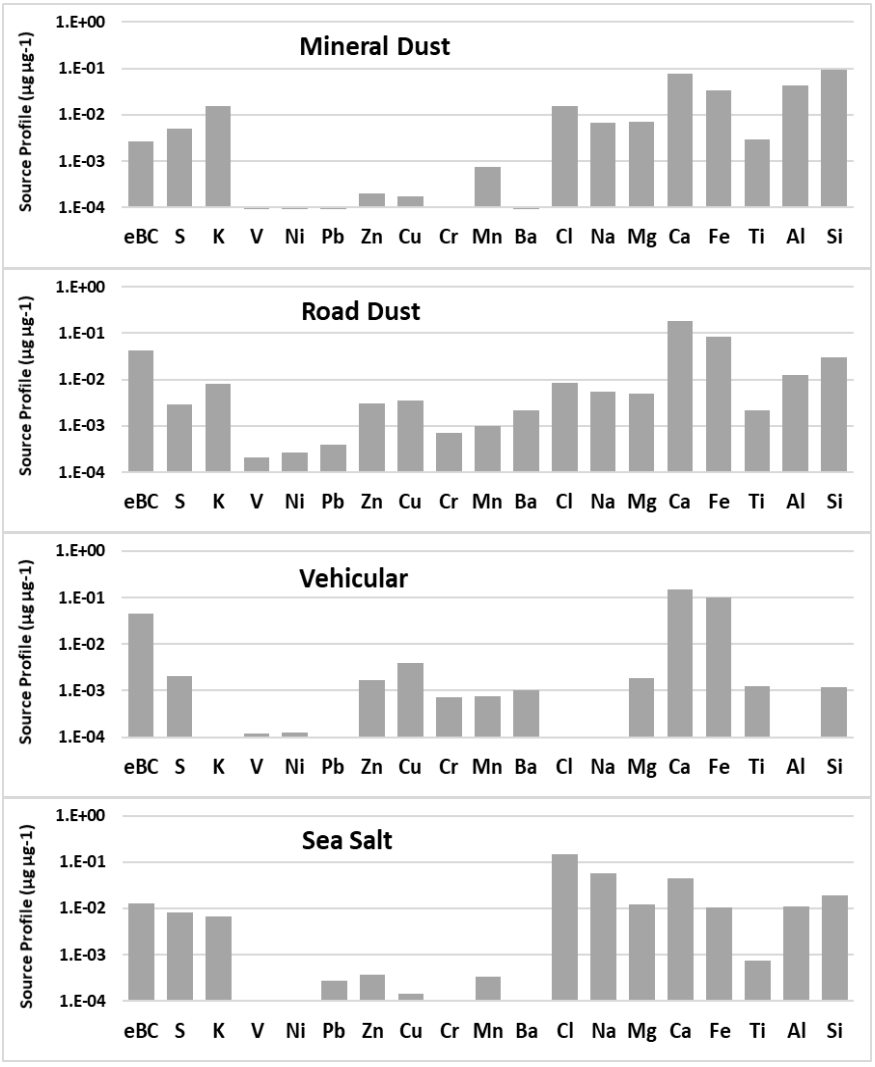

Figure S5d. PMF source profiles for $PM_{10-2.5}$ at the urban background site.

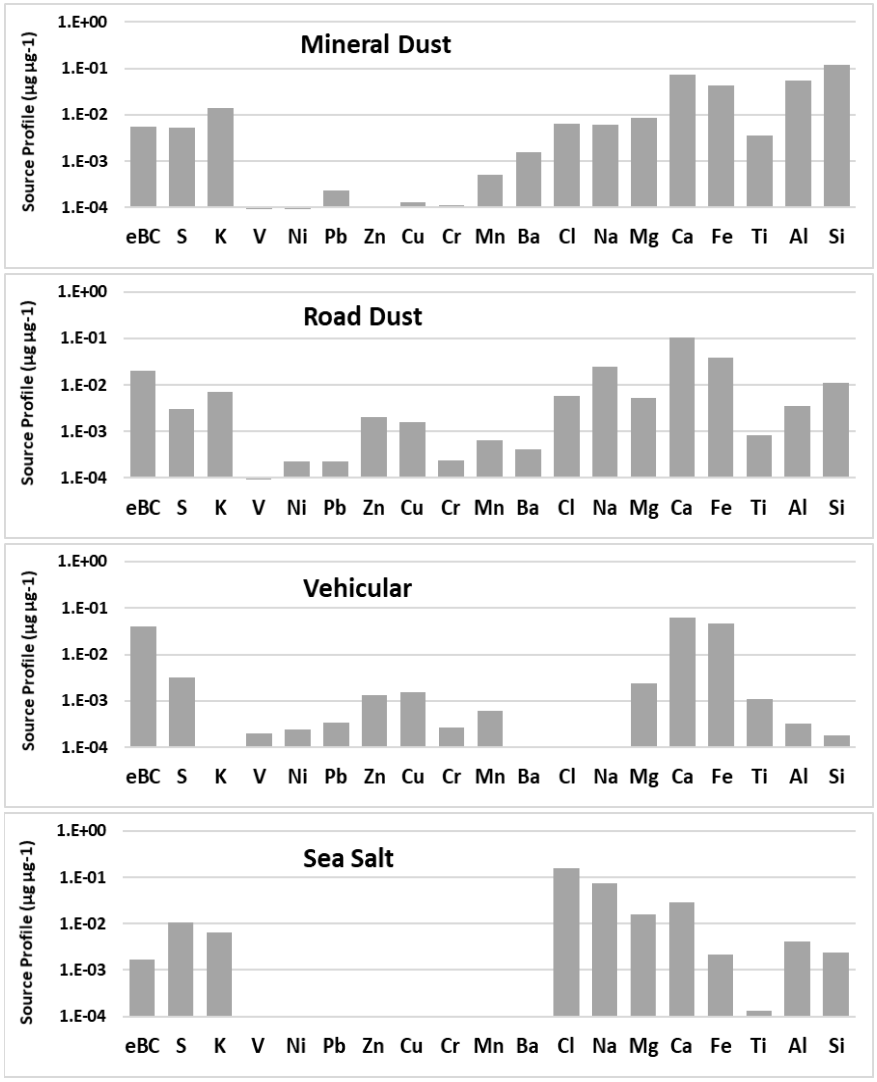

Figure S6. Clusters [a] of 4-day kinematic back-trajectories arriving at Athens, during the days of sampling (displaying also frequency of occurrence). Data table includes average PMF-estimated contributions (in μg m^{-3}) for selected factors per trajectory cluster, at the urban background site (values for the biomass burning factor calculated excluding the cold season).

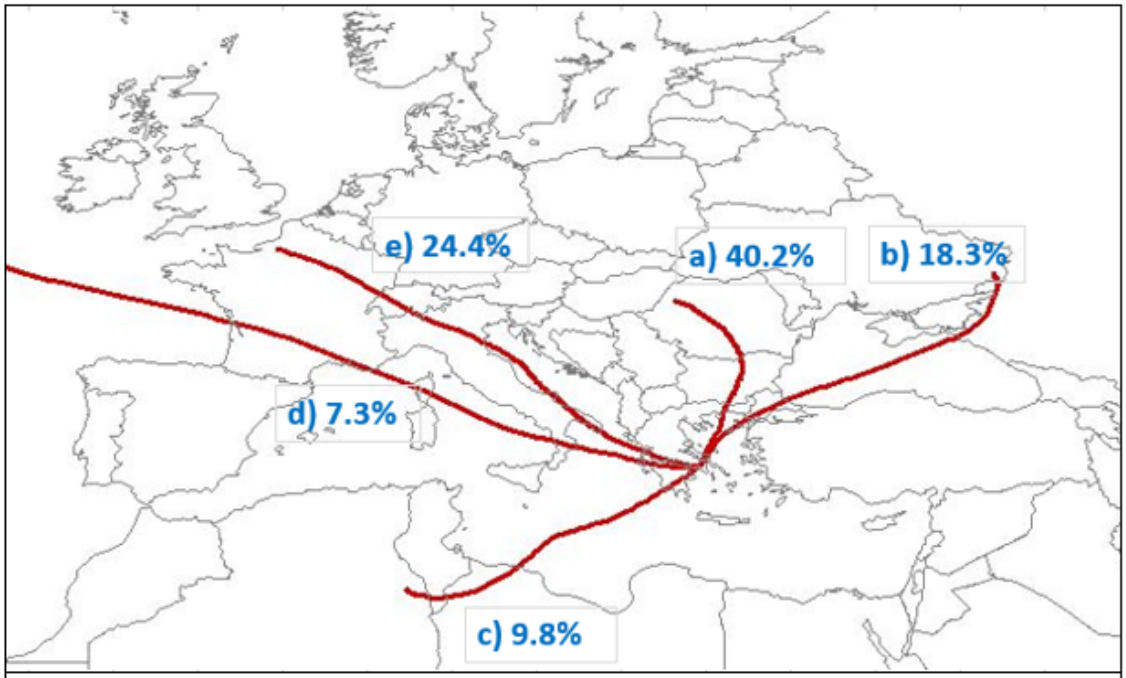

	Regional (fine)	Biomass Burning (fine)	Mineral Dust (coarse)	Sea Salt (coarse)
a) Balkans	8.8	1.8	2.8	0.3
b) Eastern Europe	10.2	1.6	4.5	0.9
c) North Africa	4.8	0.8	5.2	2.4
d) Western Mediterranean	2.5	1.1	1.3	7.7
e) Central Europe	10.7	0.4	3.8	1.0

[a] Trajectory categories were delineated by k-means clustering using Euclidean distance as the distance metric (Wang et al., 2009).

Supplementary references

Cesari, D., Contini, D., Genga, A., Siciliano, M., Elefante, C., Baglivi, F., Daniele, L., 2012. Analysis of raw soils and their re-suspended PM_{10} fractions: Characterisation of source profiles and enrichment factors. Applied Geochemistry, 27(6), pp. 1238-1246.

Grivas, G., Cheristanidis, S., Chaloulakou, A., 2012. Elemental and organic carbon in the urban environment of Athens. Seasonal and diurnal variations and estimates of secondary organic carbon. Science of the Total Environment, 414, pp. 535-545.

Wang, Y.Q., Zhang, X.Y., Draxler, R., 2009. TrajStat: GIS-based software that uses various trajectory statistical analysis methods to identify potential sources from long-term air pollution measurement data. Environmental Modeling and Software, 24, pp. 938–939.

Wedepohl, K.H., 1995. The composition of the continental crust. Geochimica Cosmochimica Acta, 59, 1217-1232.

Visser, S., Slowik, J.G., Furger, M., Zotter, P., Bukowiecki, N., Dressler, R., Flechsig, U., Appel, K., Green, D.C., Tremper, A.H., et al., 2015.Kerb and urban increment of highly time-resolved trace elements in PM_{10}, $PM_{2.5}$ and $PM_{1.0}$ winter aerosol in London during ClearfLo 2012. Atmospheric Chemistry and Physics, 15(5), pp. 2367-2386.